

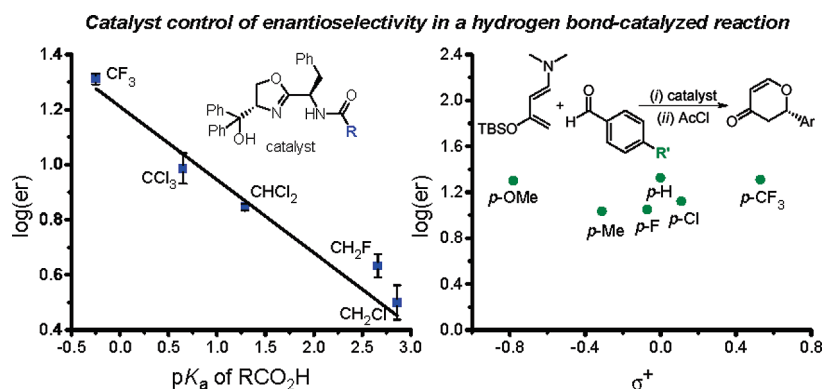
## Evaluation of Catalyst Acidity and Substrate Electronic Effects in a Hydrogen Bond-Catalyzed Enantioselective Reaction

Katrina H. Jensen and Matthew S. Sigman\*

Department of Chemistry, University of Utah, 315 South 1400 East, Salt Lake City, Utah 84112, United States

sigman@chem.utah.edu

Received July 15, 2010



A modular catalyst structure was applied to evaluate the effects of catalyst acidity in a hydrogen bond-catalyzed hetero Diels–Alder reaction. Linear free energy relationships between catalyst acidity and both rate and enantioselectivity were observed, where greater catalyst acidity leads to increased activity and enantioselectivity. A relationship between reactant electronic nature and rate was also observed, although there is no such correlation to enantioselectivity, indicating the system is under catalyst control.

### Introduction

A crucial function of hydrogen bonding in nature is transition state stabilization during enzyme catalysis. Synthetic chemists have applied this mode of activation to asymmetric catalysis, where hydrogen bond donors are used in small chiral molecules to impart facial selectivity during catalysis. Recent advancement in this field has been rapid, and a plethora of structurally distinct catalysts, covering a range of approximately 20 pK<sub>a</sub> units, have been successfully employed.<sup>1–3</sup> Despite the surge of reports, mechanistic understanding of how subtle changes to catalyst structure affect selectivity is still relatively scarce.<sup>4–7</sup> Moreover, the

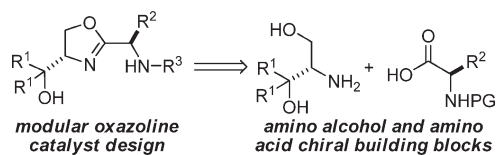
influence of catalyst acidity upon reaction outcome, both in terms of rate<sup>8,9</sup> and enantioselectivity, remains underinvestigated.<sup>10–12</sup> This lack of understanding is likely due to the fact that significant structural differences often make the direct comparison of catalysts with different acidity uninformative.

A hydrogen bond catalyst design was developed in our laboratory and consists of an oxazoline core and two pendant arms with sites capable of hydrogen bond donation (Scheme 1).<sup>13</sup> This catalyst employs amino acid derivatives as the chiral building blocks, allowing for the incorporation of a variety of substituents into the catalyst structure. A key

(1) Doyle, A. G.; Jacobsen, E. N. *Chem. Rev.* **2007**, *107*, 5713.  
 (2) Akiyama, T. *Chem. Rev.* **2007**, *107*, 5744.  
 (3) Taylor, M. S.; Jacobsen, E. N. *Angew. Chem., Int. Ed.* **2006**, *45*, 1520.  
 (4) Vachal, P.; Jacobsen, E. N. *J. Am. Chem. Soc.* **2002**, *124*, 10012.  
 (5) Zuend, S. J.; Jacobsen, E. N. *J. Am. Chem. Soc.* **2007**, *129*, 15872.  
 (6) Zuend, S. J.; Jacobsen, E. N. *J. Am. Chem. Soc.* **2009**, *131*, 15358.  
 (7) Xu, H.; Zuend, S. J.; Woll, M. G.; Tao, Y.; Jacobsen, E. N. *Science* **2010**, *327*, 986.

(8) Hine, J.; Linden, S. M.; Kanagasabapathy, V. M. *J. Am. Chem. Soc.* **1985**, *107*, 1082.  
 (9) Hine, J.; Linden, S. M.; Kanagasabapathy, V. M. *J. Org. Chem.* **1985**, *50*, 5096.  
 (10) Jensen, K. H.; Sigman, M. S. *Angew. Chem., Int. Ed.* **2007**, *46*, 4748.  
 (11) Li, X.; Deng, H.; Zhang, B.; Li, J.; Zhang, L.; Luo, S.; Cheng, J.-P. *Chem.—Eur. J.* **2010**, *16*, 450.  
 (12) Du, J.; Li, Z.; Du, D.-M.; Xu, J. *ARKIVOC* **2008**, 145.  
 (13) Rajaram, S.; Sigman, M. S. *Org. Lett.* **2005**, *7*, 5473.

## SCHEME 1. Modular Hydrogen Bond Catalyst Design



advantage of the design is its modularity, facilitating optimization of catalyst structure for a given reaction, as well as allowing systematic changes to be incorporated to advance understanding of the relationship between structure and selectivity.<sup>14,15</sup>

The viability of this general motif as a hydrogen bond catalyst was demonstrated using a model reaction, the hetero-Diels–Alder reaction<sup>16</sup> of the activated diene **1**<sup>17–20</sup> with aromatic aldehydes, initially reported by Rawal and co-workers (Figure 1).<sup>21,22</sup> The modular nature of the catalyst design allowed for the evaluation of a variety of catalyst structures, and catalyst **2** was found to provide the dihydropyranone products in high enantiomeric excess.<sup>13</sup>

Following the successful demonstration of the efficacy of the catalyst design, the focus of the project turned to utilizing the catalyst's modularity to contribute to the mechanistic understanding of enantioselective hydrogen bond catalysis. Specifically, we hoped to systematically evaluate the influence of catalyst acidity.<sup>10</sup> We hypothesized that a more acidic catalyst may lead to a stronger hydrogen bond between catalyst and aldehyde, and consequently greater substrate activation, ultimately leading to a more active catalyst. Our catalyst was seen as an ideal template with which to test this hypothesis, as its modularity allows for systematic changes to one portion of the catalyst, while keeping the remainder of the catalyst unchanged. A series of halogenated acetamide derivative catalysts **3–7** (Figure 1) was chosen, as they provide a significant range of N–H acidity (approximately 5 pK<sub>a</sub> units as measured in DMSO)<sup>23,24</sup> and all could be synthesized from a common oxazoline precursor (see Experimental Section for details). We initially reported the observation of a direct correlation between catalyst acidity and enantioselectivity in 2007.<sup>10</sup> Herein we report a more detailed investigation of this reaction, including an examination of both catalyst and substrate electronic effects on rate and enantioselectivity, and provide a plausible origin of these observations.

## Results and Discussion

Catalysts **3–7** were synthesized from a common oxazoline amine intermediate, obtained via coupling of an amino alcohol with an *N*-protected amino acid, followed by oxazoline

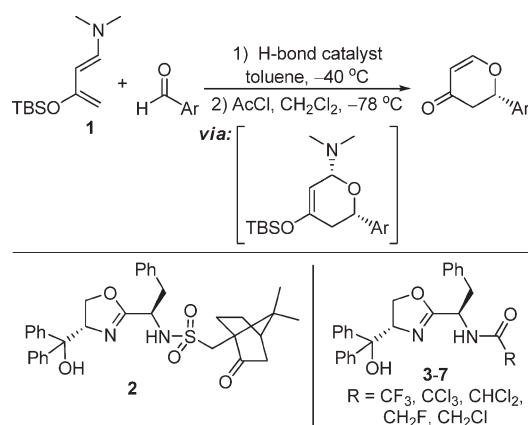


FIGURE 1. Hetero Diels–Alder reaction and modular hydrogen bond catalysts.

TABLE 1. Oxazoline-Amide Catalyzed Hetero Diels–Alder Reaction

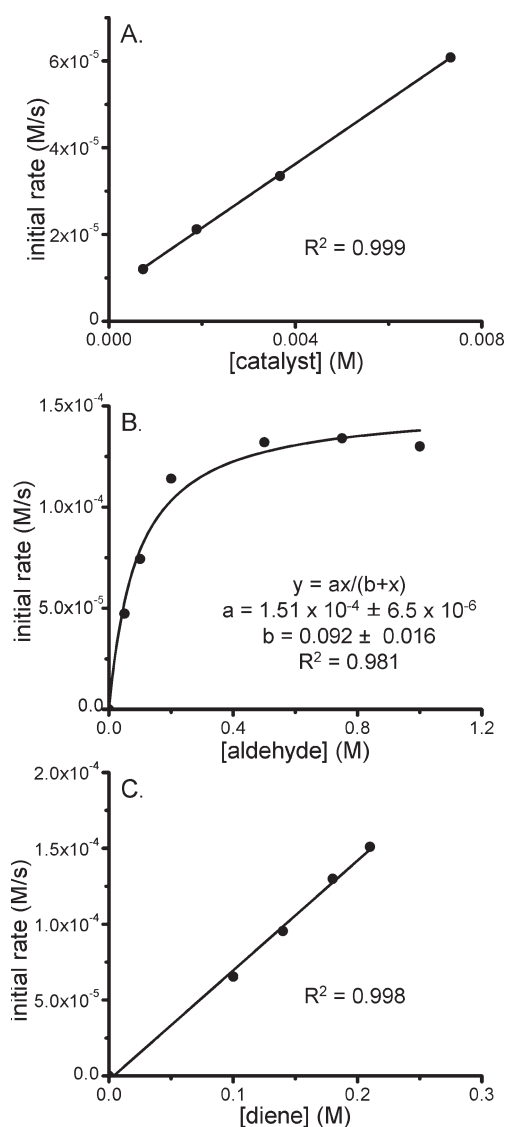
entry	catalyst	R	% yield	% ee	er
1	<b>3</b>	$\text{CF}_3$	67	91	95.3:4.7
2	<b>4</b>	$\text{CCl}_3$	61	81	90.6:9.4
3	<b>5</b>	$\text{CHCl}_2$	53	75	87.5:12.5
4	<b>6</b>	$\text{CH}_2\text{F}$	17	62	81.1:18.9
5	<b>7</b>	$\text{CH}_2\text{Cl}$	32	52	75.8:24.2

TABLE 2. Scope of Hetero Diels–Alder Reaction Catalyzed by **3**

entry	R	time (h)	temp ( $^{\circ}\text{C}$ )	% yield	% ee	er
1	Ph	60	$-65$	72	93	96:4
2	$4\text{-O}_2\text{NC}_6\text{H}_4$	48	$-65$	70	81	90:10
3	1-naphthyl	48	$-55$	74	96	98:2
4	$4\text{-ClC}_6\text{H}_4$	48	$-55$	74	83	92:8
5	$4\text{-MeOC}_6\text{H}_4$	72	$-40$	59	88	94:6
6	$\text{PhCH}=\text{CH}$	48	$-65$	65	90	95:5
7	$\text{PhCH}_2\text{CH}_2$	72	$-40$	14	47	73:27
8	$\text{CH}_3(\text{CH}_2)_4$	48	$-40$	32	30	65:35

cyclization (see Experimental Section for details). The series of catalysts was evaluated in the hetero-Diels–Alder reaction between Rawal's diene **1** and benzaldehyde **8** (Table 1). Isolated yields of the dihydropyranone product **9** were taken as the first indication that catalyst acidity may indeed affect catalytic activity, as more acidic catalysts generally gave higher product yields (Table 1). Interestingly, a trend in enantioselectivity was also observed, with the most acidic

- (14) Miller, J. J.; Sigman, M. S. *Angew. Chem., Int. Ed.* **2008**, *47*, 771.  
 (15) Sigman, M. S.; Miller, J. J. *J. Org. Chem.* **2009**, *74*, 7633.  
 (16) Pellissier, H. *Tetrahedron* **2009**, *65*, 2839.  
 (17) Huang, Y.; Rawal, V. H. *Org. Lett.* **2000**, *2*, 3321.  
 (18) Huang, Y.; Rawal, V. H. *J. Am. Chem. Soc.* **2002**, *124*, 9662.  
 (19) Kozmin, S. A.; Janey, J. M.; Rawal, V. H. *J. Org. Chem.* **1999**, *64*, 3039.  
 (20) Kozmin, S. A.; He, S.; Rawal, V. H. *Org. Synth.* **2002**, *78*, 152.  
 (21) Huang, Y.; Unni, A. K.; Thadani, A. N.; Rawal, V. H. *Nature* **2003**, *424*, 146.  
 (22) Unni, A. K.; Takenaka, N.; Yamamoto, H.; Rawal, V. H. *J. Am. Chem. Soc.* **2005**, *127*, 1336.  
 (23) Bordwell, F. G. *Acc. Chem. Res.* **1988**, *21*, 456.  
 (24) Bordwell, F. G.; Fried, H. E.; Hughes, D. L.; Lynch, T. Y.; Satish, A. V.; Whang, Y. E. *J. Org. Chem.* **1990**, *55*, 3330.

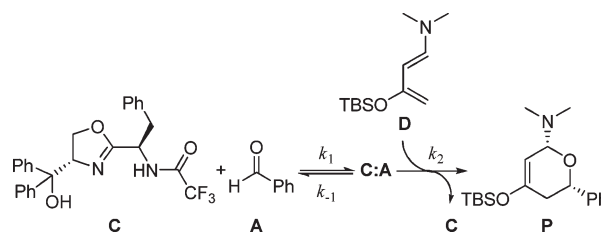


**FIGURE 2.** Reaction component dependencies with catalyst **3** measured by in situ IR spectroscopy. (A) First order dependence on [catalyst **3**], conditions: [benzaldehyde] = 0.37 M, [diene] = 0.18 M, rt. (B) Saturation in [aldehyde], conditions: [**3**] = 0.018 M, [diene] = 0.18 M, 0 °C. (C) First order dependence on [diene], conditions: [**3**] = 0.018 M, [benzaldehyde] = 1.0 M, 0 °C.

catalyst leading to the highest enantiomeric excess. This result was initially unexpected, as it was assumed that substituent size had the most significant effect on facial selectivity, and our assumption was that halogen substitution would have a minor effect upon the steric nature of the catalyst.

Because **3** was discovered to catalyze the hetero-Diels–Alder reaction with high enantioselectivity, the scope of the hetero-Diels–Alder reaction with this catalyst was examined (Table 2). In general, high enantioselectivity was obtained with aromatic aldehyde substrates (entries 1–5), highlighted by a 96% ee for 1-naphthaldehyde. An  $\alpha,\beta$ -unsaturated aldehyde, cinnamaldehyde, also gives the product in high enantiomeric excess (entry 6). Enantioselectivity is diminished for hydrocinnamaldehyde and hexanaldehyde (entries 7 and 8), but this marks an improvement as prior experimentation had shown catalyst **2** to be ineffective in the catalysis of the hetero Diels–Alder reaction with aliphatic aldehydes.

## SCHEME 2. Proposed Mechanism for the Hetero Diels–Alder Reaction Catalyzed by **3**



Thus, while the series of catalysts was initially developed as a mechanistic probe, **3** was found to be a viable catalyst. This is encouraging because **3** is significantly simpler, having fewer stereocenters and a lower molecular weight, than the camphor sulfonamide catalyst **2**.

## Mechanistic Investigation

To gain a better understanding of how the observed trends in yield and enantioselectivity based on catalyst acidity may reflect the mechanism of the reaction, kinetic measurements were acquired using in situ IR spectroscopy, and the reaction rate dependence on each reaction component was determined (Figure 2, note: rate measured by monitoring the change in IR absorbance of **1**, which is correlated to [**1**], as a function of time; rates reported in M/s). A first order dependence on [catalyst] provides evidence against a dimer or higher order species as the active catalyst (Figure 2A). Initially, kinetic measurements were performed at room temperature for practicality, but based on the observation of a nonzero intercept, indicating a background reaction, all further measurements were performed at reduced temperature (either 0 or –45 °C). Saturation in [aldehyde] was observed (Figure 2B), as well as a first order dependence on [diene] at high [aldehyde] (Figure 2C). These results led to the proposal of the mechanism shown in Scheme 2, where the catalyst and aldehyde bind reversibly to form an activated step **C:A**, which reacts with diene in the turnover limiting step to form the product.

Upon the basis of the proposed mechanism, rate law derivation was performed following the Michaelis–Menten kinetic model. Assuming the second step is the turnover determining step, the rate of product formation is proportional to the product of the concentration of the two intermediates involved in this step, where **C:A** is the activated catalyst–aldehyde complex (eq 1). As the catalyst exists in two different states in this mechanism, we define [**C**]<sub>T</sub> as the total catalyst concentration (eq 2). Using the steady state approximation (eq 3) allows us to solve for [**C:A**] (eq 4). Substitution into eq 1 results in the derived rate law (eq 5).

$$\frac{d[\text{P}]}{dt} = k_2[\text{C:A}][\text{D}] \quad (1)$$

$$[\text{C}] = [\text{C}_T] - [\text{C:A}] \quad (2)$$

$$\begin{aligned} \frac{d[\text{C:A}]}{dt} &= k_1([\text{C}_T] - [\text{C:A}])[\text{A}] - k_{-1}[\text{C:A}] \\ &\quad - k_2[\text{C:A}][\text{D}] = 0 \end{aligned} \quad (3)$$

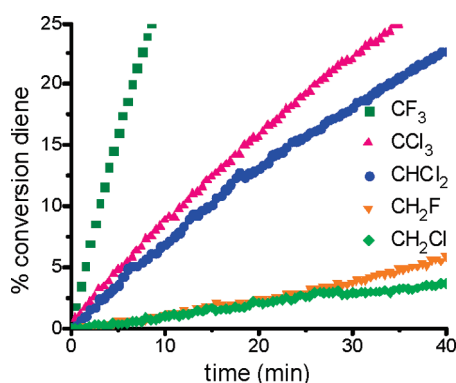


**FIGURE 3.** Conversion of diene vs time for hydrogen bond catalyst **3–7**, conditions: [benzaldehyde] = 0.78 M, [diene] = 0.18 M, [catalyst] = 0.036 M,  $-45^{\circ}\text{C}$ .

$$[\text{C} : \text{A}] = \frac{k_1[\text{C}_\text{T}][\text{A}]}{k_1[\text{A}] + k_{-1} + k_2[\text{D}]} \quad (4)$$

$$\frac{d[\text{P}]}{dt} = \frac{k_1 k_2 [\text{C}_\text{T}][\text{A}][\text{D}]}{k_1[\text{A}] + k_{-1} + k_2[\text{D}]} \quad (5)$$

Importantly, the derived rate law is consistent with the empirical observations. Specifically, when [aldehyde] is low the rate law can be simplified to eq 6 which is consistent with a first order dependence of rate on [aldehyde], and when [aldehyde] is high the rate law can be simplified to eq 7 which is consistent with zero order dependence of rate on [aldehyde], and first order dependence on [catalyst] and [diene].

$$\frac{d[\text{P}]}{dt} = \frac{k_1 k_2 [\text{C}_\text{T}][\text{A}][\text{D}]}{k_{-1} + k_2[\text{D}]} \quad (6)$$

$$\frac{d[\text{P}]}{dt} = k_2 [\text{C}_\text{T}][\text{D}] \quad (7)$$

### Catalyst Acidity Effects

In light of the proposed mechanism, the question remained whether catalyst acidity is affecting the binding equilibria of catalyst with substrate ( $k_1/k_{-1}$ ), the rate of reaction of the activated aldehyde **C:A** with diene ( $k_2$ ), or both. To determine the influence upon the second step, the reaction rate was measured for the complete series of catalysts **3–7** under saturation conditions. A clear trend was observed, with the most acidic catalyst leading to the highest rate (Figure 3).

To determine whether this trend in reaction could be directly correlated to the electronic nature of the catalyst, a Brønsted-type plot was constructed (Figure 4). The Brønsted equation (eq 8)<sup>25</sup> relates the rate of an acid-catalyzed reaction to the  $\text{p}K_\text{a}$  of the corresponding acid. The resulting linear free energy relationship is similar to the more common Hammett relationship, where  $\text{p}K_\text{a}$ 's of benzoic acids are used as the reference measurement for the effect of electronic perturbations on rate or equilibrium. In our case, we chose to

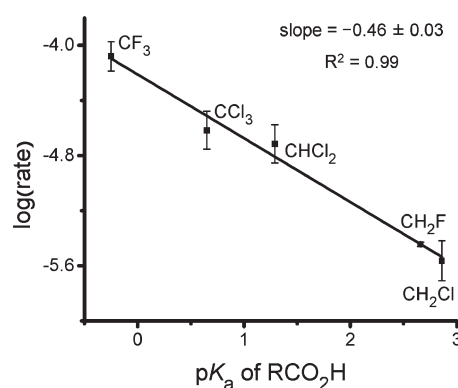


**FIGURE 4.** Linear free energy relationship between rate and  $\text{p}K_\text{a}$  of the corresponding acetic acid derivative, conditions: [benzaldehyde] = 0.78 M, [diene] = 0.18 M, [catalyst] = 0.036 M,  $-45^{\circ}\text{C}$ .

use the  $\text{p}K_\text{a}$  values of acetic acid derivatives measured in water as the reference, with the key assumption being that the electron-withdrawing ability of the R substituent affects the acidity of our catalyst and the acidity of the corresponding acetic acid derivative similarly.

$$\log(k) = -\alpha(\text{p}K_\text{a}) + C \quad (8)$$

To evaluate the effect of catalyst acidity upon substrate binding, the saturation curves for the most and least acidic catalysts, **3** and **7**, respectively, were examined (Figure 5, note y-axis scales are different). Comparing the curvature of these two plots, saturation is reached at much lower [aldehyde] for the more acidic catalyst (Figure 5A) than for the least acidic catalyst (Figure 5B), indicating that binding equilibrium is also perturbed by catalyst acidity.

With the understanding that catalyst acidity has a direct effect on both substrate binding and rate of reaction with diene, we were interested in whether the observed trends in enantioselectivity could also be directly correlated to catalyst acidity. Considering that enantiomeric ratio is a measurement of the relative rate of formation of each enantiomer ( $\text{er} = k_\text{S}/k_\text{R}$ ), a Brønsted-type plot was constructed by plotting  $\log(\text{er})$  vs  $\text{p}K_\text{a}$  (Figure 6). A linear free energy relationship was observed between enantioselectivity and acidity, a unique example of such a direct correlation in a hydrogen bond catalyzed reaction. This indicates that enantioselectivity can be directly perturbed by the hydrogen bond donating ability.

### Substrate Electronic Effects

In an attempt to further understand the subtleties of the system, we chose to evaluate the influence of substrate electronic perturbations. We hypothesized that the electronic nature of the substrate could potentially affect both the rate at which the aldehyde reacts with the diene, as well as the Lewis basicity and thus the binding of substrate to catalyst. Therefore, a series of benzaldehyde derivatives with either electron-donating or electron-withdrawing substituents in the *para* position were examined. In situ IR was used to monitor the rate of the reaction. We first examined the two most electronically disparate cases within the series, *p*-anisaldehyde **10** and *p*-trifluoromethylbenzaldehyde **11**. Initial reaction rates were measured over a range of [aldehyde]. Similar rates were observed at low [aldehyde],

(25) Anslyn, E. V.; Dougherty, D. A. *Modern Physical Organic Chemistry*; University Science Books: Sausalito, CA, 2006; p 466.

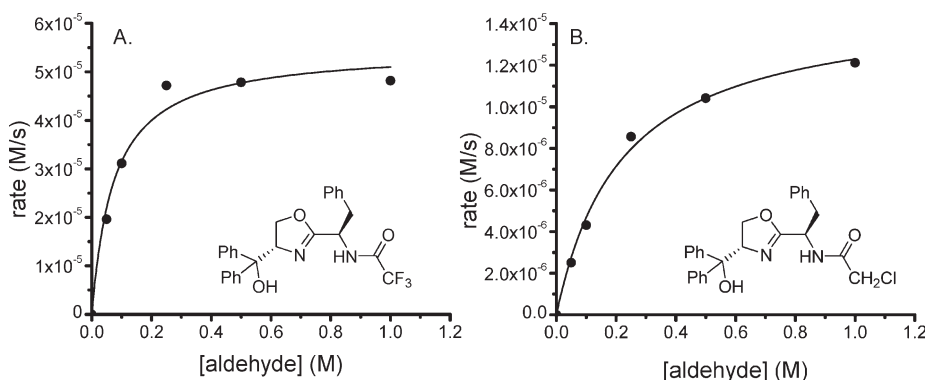


**FIGURE 5.** Comparison of saturation in [aldehyde] for catalysts **3** and **7**. Conditions: [diene] = 0.075 M, [catalyst] = 0.018 M,  $-45\text{ }^{\circ}\text{C}$ . Fit to  $y = ax/(b + x)$ . (A)  $a = 5.47 \times 10^{-5} \pm 3.1 \times 10^{-6}$ ,  $b = 0.074 \pm 0.017$ ,  $R^2 = 0.97$ ; (B)  $a = 1.45 \times 10^{-5} \pm 6.4 \times 10^{-7}$ ,  $b = 0.209 \pm 0.029$ ,  $R^2 = 0.99$ .

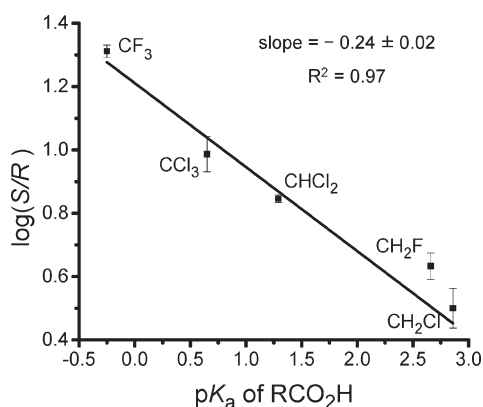


**FIGURE 6.** Linear free energy relationship between enantiomeric ratio and  $pK_a$  of the corresponding acetic acid derivative, conditions: [benzaldehyde] = 0.36 M, [diene] = 0.18 M, [catalyst] = 0.036 M,  $-40\text{ }^{\circ}\text{C}$ .

however, significant differences can be observed in the saturation curves for the two substrates. *p*-Anisaldehyde reaches saturation at a lower [aldehyde] (Figure 7A), as would be expected with a more electron rich aldehyde which is a stronger Brønsted base and thus binds to the catalyst more effectively. On the other hand, *p*-trifluoromethylbenzaldehyde achieves a much higher rate of reaction at saturation (Figure 7B), which is consistent with this being the more electron-poor, and thus more electrophilic aldehyde.

The rate of the hydrogen bond-catalyzed hetero-Diels–Alder reaction was measured at both high and low [aldehyde] with a series of benzaldehyde derivatives bearing electron-donating or electron-withdrawing substituents (Table 3). A Hammett plot was constructed by plotting  $\log(\text{rate})$  vs  $\sigma^+$  (Figure 8). When [aldehyde] = 1.0 M (conditions where saturation is assumed) a linear free energy correlation is observed, with  $\rho^+ = 1.61 \pm 0.16$  (Figure 8A).<sup>26</sup> A positive  $\rho$  value indicates that there is a build up of negative charge, or diminution of positive charge, during the transition state. Additionally, the better fit obtained with  $\sigma^+$  than with  $\sigma$  indicates significant resonance contribution from electron donating groups. This is consistent with the proposed

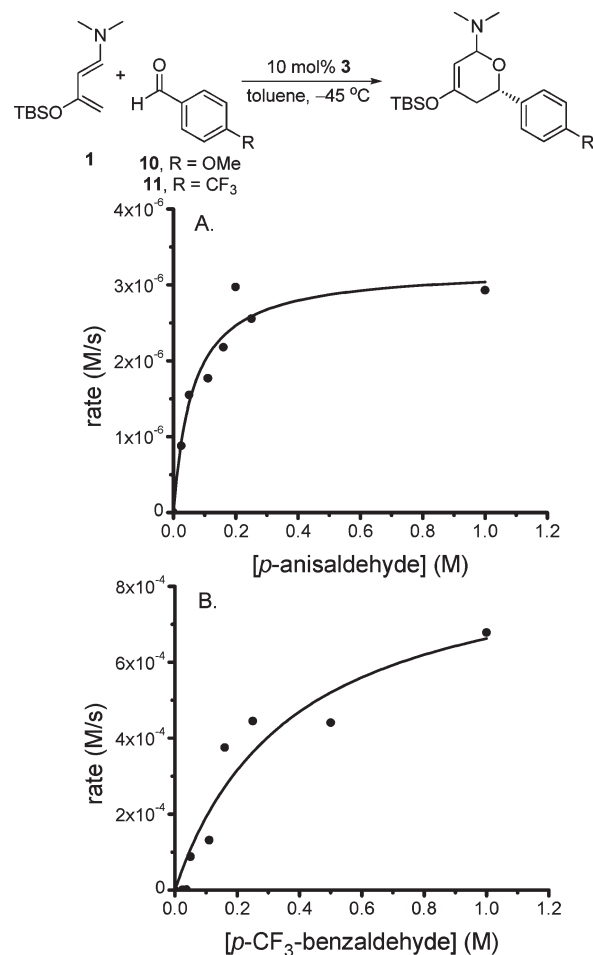


**FIGURE 7.** [aldehyde] saturation curves for benzaldehyde derivatives bearing (A) an electron-donating group and (B) an electron-withdrawing group. Conditions: [catalyst **3**] = 0.016 M, [diene] = 0.16 M,  $-45\text{ }^{\circ}\text{C}$ .

mechanism in which a hydrogen bond is formed between aldehyde and catalyst, which would lead to a build up of positive charge on the carbonyl carbon of the aldehyde. Stabilization of this positive charge by electron donation would lead to a lower energy C:A intermediate, as demonstrated by the difference in saturation curves in Figure 7. A lower energy for the C:A intermediate would contribute to a

(26) Rate data for 4-Cl-benzaldehyde and 4-Br-benzaldehyde were not obtained at high [aldehyde] due to poor solubility of these substrates at reduced temperature.

TABLE 3. Rate of Hetero Diels–Alder Reaction Catalyzed by **3**<sup>a</sup>

R	$\sigma^+$	[aldehyde] = 1.0 M		[aldehyde] = 0.025 M	
		average rate (M/s)	log(rate)	average rate (M/s)	log(rate)
CF <sub>3</sub>	0.53	$6.78 \times 10^{-4}$	-3.17	$6.35 \times 10^{-7}$	-6.20
Br	0.15	—	—	$1.87 \times 10^{-5}$	-4.73
Cl	0.11	—	—	$1.54 \times 10^{-5}$	-4.83
H	0	$4.64 \times 10^{-5}$	-4.43	$6.03 \times 10^{-6}$	-5.22
F	-0.07	$2.93 \times 10^{-5}$	-4.53	$6.51 \times 10^{-6}$	-5.19
Me	-0.31	$2.61 \times 10^{-5}$	-4.58	$2.90 \times 10^{-6}$	-5.54
OMe	-0.78	$2.93 \times 10^{-6}$	-5.53	$8.21 \times 10^{-7}$	-6.09

<sup>a</sup>Conditions: [catalyst] = 0.016 M, [diene] = 0.16 M, -45 °C.

TABLE 4. Enantiomeric Excess of Hetero Diels–Alder Adducts with Benzaldehyde Derivatives

entry	R	% ee	er
1	CF <sub>3</sub>	91	95.4:4.6
2	Cl	86	93.0:7.0
3	F	84	91.8:8.2
4	H	91	95.5:4.5
5	Me	83	91.5:8.5
6	OMe	90	95.2:4.8

in mechanism as this aldehyde substrate is such a poor Brønsted base that  $k_1$  is turnover limiting.

The observed Hammett correlation under saturation conditions is consistent with previous LFERs observed for other Diels–Alder reactions.<sup>27–35</sup> In general positive  $\rho$  values are observed with respect to electronic perturbations to the dienophile, whereas negative  $\rho$  values are observed when derivatives of the diene are examined. This is in agreement with the generally accepted view of a polar, asynchronous [4 + 2] cycloaddition pathway in which the diene and the dienophile can be considered the nucleophile and the electrophile, respectively.

Inspection of the enantiomeric excess of the products formed following workup with acetyl chloride shows no effect of the electronic nature of the aldehyde upon enantioselectivity (Table 4). Plotting log(er) vs either  $\sigma$  or  $\sigma^+$  shows no LFER (Figure 9). This indicates that the enantioselectivity of the reaction is solely under catalyst control (vide infra).

#### Origin of Catalyst Acidity Effect on Enantioselectivity

The observation of such direct effects of catalyst acidity on both rate and enantioselectivity should prove beneficial in the future design of hydrogen bond catalysts for asymmetric catalysis. While the effect upon rate was expected, the direct effect on enantioselectivity was not. Several explanations to account for such an effect can be proposed.

One explanation might be that a background, or uncatalyzed reaction, is occurring concurrent to the catalyzed reaction. This uncatalyzed reaction would result in racemic product, and thus the overall enantiomeric excess of product would be diminished. As  $k_{\text{cat}}$  decreases, the effect of a background reaction would certainly be more significant. In the case of our system, however, the background reaction at -45 °C is not significant with no product formation observed after 48 h at this temperature. Furthermore, this explanation is

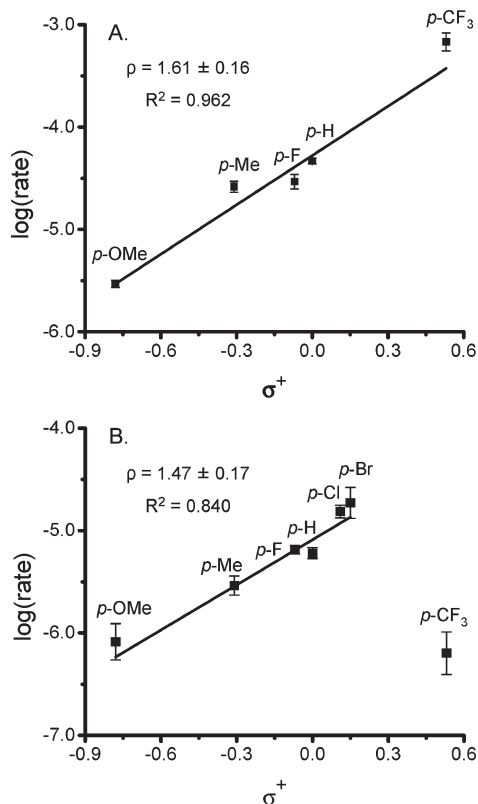


FIGURE 8. Hammett plots relating aldehyde electronic nature and reaction rate. Conditions: [catalyst **3**] = 0.016 M, [diene] = 0.16 M, -45 °C. (A) [aldehyde] = 1.0 M, (B) [aldehyde] = 0.025 M.

higher activation energy for electron rich benzaldehyde derivatives, as evidenced by the decrease in  $k_2$ .

When [aldehyde] = 0.025 M, again a linear free energy relationship is observed using  $\sigma^+$  values with a  $\rho$  value of 1.47. However, a break in the Hammett plot is observed when evaluating the most electron poor aldehyde (Figure 8B). On the left-hand side,  $\rho$  is positive as the substrates are electron rich enough to be in a situation where  $k_2$  is turnover limiting. In contrast, with a very electron withdrawing substituent, it is likely that there is a change in turnover limiting step or change

(27) Doyle, M. P.; Valenzuela, M.; Huang, P. *Proc. Natl. Acad. Sci. U.S.A.* **2004**, *101*, 5391.

(28) Benghait, I.; Becker, E. I. *J. Org. Chem.* **1958**, *23*, 885.

(29) Lotfi, M.; Roberts, R. M. G. *Tetrahedron* **1979**, *35*, 2131.

(30) Okamoto, Y.; Brown, H. C. *J. Org. Chem.* **1957**, *22*, 485.

(31) DeWitt, E. J.; Lester, C. T.; Ropp, G. A. *J. Am. Chem. Soc.* **1956**, *78*, 2101.

(32) Inukai, T.; Kojima, T. *J. Chem. Soc. D* **1969**, 1334.

(33) Salakhov, M. S.; Musaeva, N. F.; Suleimanov, S. N. *Org. React. (Tartu)* **1979**, *16*, 54.

(34) Domingo, L. R.; Saez, J. A. *Org. Biomol. Chem* **2009**, *7*, 3576.

(35) Charton, M. *J. Org. Chem.* **1966**, *31*, 3745.

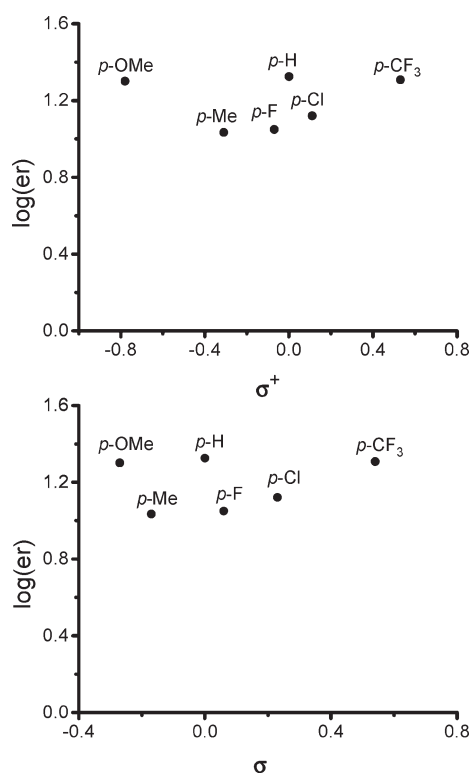


**FIGURE 9.** Hammett plots show no linear free energy relationship for enantioselectivity, conditions: [benzaldehyde] = 0.36 M, [diene] = 0.18 M, [catalyst] = 0.036 M,  $-45\text{ }^{\circ}\text{C}$ .

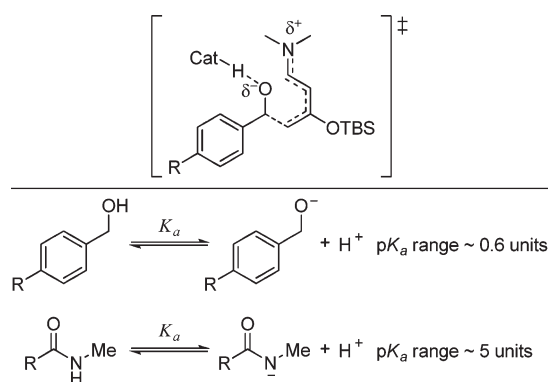


**FIGURE 10.** Effect of substituents on acidity of hydrogen bond donor and acceptor in proposed the transition state.

inconsistent with the lack of a correlation between substrate electronic nature and enantioselectivity.

A reasonable explanation is that a stronger hydrogen bond between the catalyst and the substrate at the transition state is formed with the more acidic catalyst, leading to increased rigidity in the transition state. It has been reported that if the  $pK_a$  of the hydrogen bond donor and that of the protonated hydrogen bond acceptor are closely matched, a shorter and stronger hydrogen bond is formed.<sup>36–38</sup> While the  $pK_a$  difference between catalyst and protonated substrate is substantial, they are more closely matched with a more

acidic catalyst. Furthermore, this disparity likely decreases in the transition state, as negative charge builds on the carbonyl oxygen. The formation of a stronger hydrogen bond in the transition state may lead to greater rigidity, and thus account for the higher enantioselectivity observed with more acidic catalysts. In contrast, there is a lack of correlation between substrate electronic nature and enantioselectivity (Table 4). When considering a possible transition state structure, the substrate portion, with negative charge on the oxygen atom stabilized by hydrogen bond formation to the catalyst, is analogous to the conjugate base of benzyl alcohol (Figure 10). The  $pK_a$  range of *para*-substituted benzylic alcohols is quite small (approximately 0.6  $pK_a$  units, a 4-fold difference in  $K_a$ ),<sup>39</sup> and thus has less of an impact on the strength of hydrogen bond formed in the transition state than the catalyst, where the range is significant (approximately 5  $pK_a$  units, a  $10^5$ -fold difference in  $K_a$ ).<sup>23,24</sup>

## Conclusion

We have presented a detailed examination of the effect of catalyst acidity in an enantioselective hydrogen bond-catalyzed reaction. This systematic study investigates the effects of electronic perturbations to both the catalyst and substrate. A process where catalyst acidity controls enantioselectivity is revealed. Since our initial report of a direct correlation between catalyst acidity and enantioselectivity,<sup>10</sup> examples of similar trends in other hydrogen bond-catalyzed reactions have emerged,<sup>11,12</sup> implying this effect is not unique to our system. However, ideal catalyst acidity is likely to differ depending on the specific reaction of interest, as the role of the catalyst is to stabilize the transition state more than the bound substrate intermediate, therefore it should not be assumed that a more acidic catalyst will always lead to improved enantioselectivity.<sup>40</sup> Optimal matching of the  $pK_a$ 's of catalyst and transition state structure should lead to improved catalyst performance in other systems as well, and the understanding gained in this study may aid in future catalyst design.

## Experimental Section

**Preparation of Catalyst 3 (2,2,2-Trifluoro-*N*-((*R*)-1-((*S*)-4-(hydroxydiphenylmethyl)-4,5-dihydrooxazol-2-yl)-2-phenylethyl)-acetamide).** The synthesis of the Cbz oxazoline intermediate (benzyl (*R*)-1-((*S*)-4-(hydroxydiphenylmethyl)-4,5-dihydrooxazol-2-yl)-2-phenylethylcarbamate) **12** has been previously reported.<sup>13</sup> A 100 mL round-bottom flask was charged with 44 mg of 10% Pd/C and the flask was flushed with nitrogen. In a separate 100 mL flask, 442.3 mg of oxazoline **12** (0.873 mmol) was dissolved in 6 mL of dry MeOH, and this solution was transferred via cannula into the flask containing Pd/C (on occasions when this is difficult, gentle warming or addition of excess MeOH is helpful and has no discernible effect on overall yield). A further 4 mL of MeOH ( $2 \times 2$  mL) was used for rinsing. The flask was then evacuated under water aspirator pressure and filled with  $\text{H}_2$  from a balloon. The cycle was repeated thrice more, and the reaction mixture was stirred under a  $\text{H}_2$  balloon atmosphere. On completion of reaction (7–8 h, by disappearance of oxazoline **12** on TLC,  $R_f = 0.6$  with 1:1 EtOAc/hexanes), the reaction mixture was filtered through a pad

(36) Perrin, C. L. *Science* **1994**, *266*, 1665.

(37) Cleland, W. W.; Kreevoy, M. M. *Science* **1994**, *264*, 1887.

(38) Schwartz, B.; Drucekhammer, D. G.; Usher, K. C.; Remington, S. J. *Biochemistry* **1995**, *34*, 15459.

(39) Based on calculated  $pK_a$  values reported on Scifinder (Calculated using Advanced Chemistry Development Software V8.14).

(40) Davis, T. A.; Wilt, J. C.; Johnston, J. N. *J. Am. Chem. Soc.* **2010**, *132*, 2880.

of Celite. The filtrate was concentrated under reduced pressure, and the resulting residue was dissolved in benzene and concentrated under reduced pressure to remove exogenous water ( $2 \times 30$  mL benzene), then dried overnight under high vacuum and used without further purification. The residue from deprotection was dissolved in 5 mL of dry  $\text{CH}_2\text{Cl}_2$  under nitrogen along with 10.7 mg of DMAP (0.087 mmol, 0.10 equiv). To this solution, 490  $\mu\text{L}$  of freshly distilled  $\text{Et}_3\text{N}$  (3.49 mmol, 4 equiv) was added. The reaction mixture was cooled to  $0^\circ\text{C}$  in an ice bath. In a separate flask, 123  $\mu\text{L}$  of trifluoroacetic anhydride (95% pure, 0.873 mmol, 1 equiv) was dissolved in 3 mL of  $\text{CH}_2\text{Cl}_2$ . This solution was transferred via cannula into the reaction flask. An additional 2 mL of  $\text{CH}_2\text{Cl}_2$  was used for rinsing. The reaction mixture was stirred for 4 h, then diluted with 30 mL of  $\text{CH}_2\text{Cl}_2$  and washed with 30 mL of saturated aqueous  $\text{NaHCO}_3$  followed by 30 mL of brine. The organic phase was dried over  $\text{Na}_2\text{SO}_4$ , filtered, and concentrated. The crude mixture in a minimum amount of  $\text{CH}_2\text{Cl}_2$  was purified by flash silica-gel column chromatography with 20 to 25 to 30%  $\text{Et}_2\text{O}$ /hexanes as the solvent to give 178.8 mg of **3** (yield: 43%).  $R_f = 0.7$  with 1:1 EtOAc/hexanes; white solid; mp:  $50\text{--}52^\circ\text{C}$ ;  $[\alpha]_{\text{D}}^{20} = -20$  ( $c = 0.28$ ,  $\text{CHCl}_3$ );  $^1\text{H NMR}$  (300, MHz  $\text{CD}_2\text{Cl}_2$ )  $\delta = 2.50$  (s, 1 H), 3.10 (dd,  $J = 6.6, 14.0$  Hz, 1 H), 3.23 (dd,  $J = 6.0, 14.0$  Hz, 1 H), 4.26 (d,  $J = 8.9$  Hz, 1 H), 4.27 (d,  $J = 8.9$  Hz, 1 H), 4.81 (ddd,  $J = 6.0, 6.5, 6.5$  Hz, 1 H), 5.25 (dd,  $J = 8.9, 8.9$  Hz, 1 H), 6.79 (br d,  $J = 6.0$  Hz, 1 H), 7.13–7.37 (m, 11 H), 7.41–7.46 (m, 4 H).  $^{13}\text{C NMR}$  (75 MHz,  $\text{CD}_2\text{Cl}_2$ )  $\delta = 37.5, 50.0, 70.8, 73.2, 78.6, 115.8$  (q,  $J = 288$  Hz), 126.0, 126.5, 127.3, 127.5, 127.8, 128.4, 128.7, 129.1, 129.6, 135.3, 144.2, 145.9, 157.0 (q,  $J = 38$  Hz), 167.1. IR: (KBr) 3482, 3393, 3062, 3030, 2360, 2343, 1721, 1668, 1543, 1496, 1449, 1210, 1173, 749,  $700\text{ cm}^{-1}$ . HRMS  $\text{C}_{26}\text{H}_{23}\text{F}_3\text{N}_2\text{O}_3$   $m/z$  ( $\text{M}+\text{Na}$ ) $^+$  calcd 491.1558, obsvd 491.1557.

Synthesis of catalyst **4–7** follows an analogous procedure to that described above for **3**. See Supporting Information for full characterization data.

**Standard Procedure for the Hetero Diels–Alder Reaction.** All pyranone products were prepared according to the following representative procedure: to an oven-dried 4 mL vial with a septum cap containing 20.6 mg of **3** (0.0440 mmol, 0.200 equiv) under nitrogen, 500  $\mu\text{L}$  of dry toluene was added followed by 45  $\mu\text{L}$  of benzaldehyde (0.44 mmol, 2 equiv). The vial was cooled to  $-40^\circ\text{C}$  and 50 mg of diene **1** (0.22 mmol, 1 equiv) dissolved in 500  $\mu\text{L}$  of toluene was transferred via cannula into

the reaction vial. An additional 200  $\mu\text{L}$  of toluene was used for rinsing. After stirring for 48 h at  $-40^\circ\text{C}$ , the reaction mixture was cooled to  $-78^\circ\text{C}$ , diluted with 2 mL of  $\text{CH}_2\text{Cl}_2$ , and 31  $\mu\text{L}$  of acetyl chloride (0.44 mmol, 2 equiv) was added. After stirring for 30 min, the contents were directly transferred to a silica column for purification using 5–15% EtOAc/hexanes as eluent to give 26.1 mg of **9**. Yield: 67%; yellow oil. The  $^1\text{H NMR}$  of the pyranone products were compared to those reported previously.<sup>22,41,42</sup>

**Standard in situ FTIR Procedure.** The ASI React IR 1000 or the Mettler Toledo React IR ic10 was used to analyze reaction progress in situ. For each reaction, the probe was cleaned and a background spectrum was taken. Disappearance of diene **1** was observed by recording the absorbance at maximum peak height ( $1648.2\text{ cm}^{-1}$  for ASI React IR 1000 or  $1649.6\text{ cm}^{-1}$  Mettler Toledo React IR ic10). The absorbance measurements were converted to concentration units dividing by the constant ( $\epsilon = 1.0885$  or  $\epsilon = 0.769$ ) relating absorbance to concentration determined by constructing calibration curves of the starting materials (Beer's Law). The apparatus used was a 50 mL Schlenk flask with a sidearm and a 24/40 ground glass joint for probe insertion. An ice water bath was used for reactions performed at  $0^\circ\text{C}$ . A dry ice/MeCN bath was used for reactions performed at  $-45^\circ\text{C}$ . Standard solutions of catalyst, aldehyde, and diene were used. Each kinetic experiment was conducted similar to this example procedure: the probe was equipped with a 50 mL Schlenk flask fitted with a stirbar, and the flask was flushed with nitrogen. To the apparatus are added 241  $\mu\text{L}$  of 0.076 M solution of **3** (0.018 mmol), 400  $\mu\text{L}$  of 2.50 M solution of benzaldehyde **8** (1.00 mmol), and 192  $\mu\text{L}$  of toluene. The reaction flask was placed in an ice bath and allowed to stir for approximately 20 min. The IR instrument was programmed to collect spectra every 15 or 30 s. Following commencement of data collection, 167  $\mu\text{L}$  of 1.10 M solution of diene **1** (0.183 mmol) was added and data collection was continued for 1–6 h. Initial rates were determined after 5% conversion of diene.

**Acknowledgment.** This work was supported by the National Science Foundation (CHE-0749506). MSS thanks the Dreyfus Foundation (Teacher-Scholar) and Pfizer for their support.

**Supporting Information Available:** Experimental procedures, kinetic data, and full spectroscopic data for all new compounds. This material is available free of charge via the Internet at <http://pubs.acs.org>.

(41) Ji, B.; Yuan, Y.; Ding, K.; Meng, J. *Chem.—Eur. J.* **2003**, *9*, 5989.  
(42) Schaus, S. E.; Branalt, J.; Jacobsen, E. N. *J. Org. Chem.* **1998**, *63*, 403.